

# Compartmental model with loss of immunity: analysis and parameters estimation for Covid-19

Cristiane M. Batistela<sup>a</sup>, Diego P. F. Correa<sup>b</sup>, Átila M Bueno<sup>c</sup>, José R. C. Piqueira<sup>a,\*</sup>

<sup>a</sup>*Polytechnic School of University of Sao Paulo - EPUSP, São Paulo, SP, Brazil.*

<sup>b</sup>*Federal University of ABC - UFABC, São Bernardo do Campo, SP, Brazil*

<sup>c</sup>*São Paulo State University - UNESP, Sorocaba, SP, Brazil*

---

## Abstract

The outbreak of Covid-19 led the world to an unprecedented health and economical crisis. In an attempt to responde to this emergency researchers worldwide are intensively studying the Covid-19 pandemic dynamics. In this work, a SIRSi compartmental model is proposed, which is a modification of the known classical SIR model. The proposed SIRSi model considers differences in the immunization within a population, and the possibility of unreported or asymptomatic cases. The model is adjusted to three major cities of São Paulo State, in Brazil, namely, São Paulo, Santos and Campinas, providing estimates on the duration and peaks of the outbreak.

*Keywords:* Covid-19, Compartmental models, Equilibrium analysis, Parameter fitting.

---

## 1. Introduction

The Wuhan Municipal Health Commission reported a cluster of 27 pneumonia cases on 31st December 2019, in the Wuhan city, Hubei Province in China. On 1st January 2020 the World Health Organization (WHO) set up the Incident Management Support Team putting the organization to an emergency level for

---

\*Corresponding author

*Email addresses:* [cmbatistela@yahoo.com.br](mailto:cmbatistela@yahoo.com.br) (Cristiane M. Batistela), [diego.ferruzzo@ufabc.edu.br](mailto:diego.ferruzzo@ufabc.edu.br) (Diego P. F. Correa), [atila.bueno@unesp.br](mailto:atila.bueno@unesp.br) (Átila M Bueno), [piqueira@lac.usp.br](mailto:piqueira@lac.usp.br) (José R. C. Piqueira)

dealing with the outbreak. On 5th January 2020 WHO published the first outbreak news on the new virus. On 7th January the causative agent was identified and named Severe Acute Respiratory Syndrome Coronavirus 2 (SARS-CoV-2) (WHO named the disease Covid-19). On 13th January 2020 the first case outside China was reported in Thailand. On 22nd January 2020 WHO stated that there was evidence of human-to-human transmission, and approximately seven weeks later, on 13th March 2020, WHO characterized the Covid-19 as a pandemic [1, 2].

In Brazil, the first confirmed Covid-19 case was reported on the 26th February 2020, and up to 25th June 2020 there was 1,188,631 confirmed cases with 53,830 deaths [3]. Globally, according to [4] there was 9,292,202 confirmed cases, and 479,133 deaths up to 25th June 2020<sup>1</sup>.

Most cases are asymptomatic carriers and are spontaneously resolved, however, some developed various fatal complications, notably for patients with comorbidities [2], and, allied to the fastly spread of covid-19, the worldwide emergency state brings up with important, and yet unanswered, questions related to the contagion dynamical behavior and its mitigation and control strategies. As a result, strategies to contain the contagion such as social distancing, quarantine and complete lockdown of areas have been studied [5, 6, 7, 8, 9, 10]

In Mexico, on 18th March 2020, the Mexican Health Secretariat reported that the pandemic was going to last 90 days, with 250,656 expected cases. On the next day, the Health Secretariat informed that approximately 9.8% (24,594) of the cases would need hospitalization, and 4.2% (10,528) of the total cases would be critical patients, needing intensive care. On the same date the number of available Health Care units at that time was 4,291 with 2,053 ventilators [11]. The situation in Mexico led to the adoption of non-pharmaceutical interventions, such as washing hands, social distancing, cough/sneeze etiquette, and so on.

In Rio de Janeiro, Brazil, the social distancing started on 17 March 2020 [8], and the government of the state of São Paulo, Brazil, decreed quarantine on

---

<sup>1</sup>Reported on 2:25pm CEST.

23rd March 2020. Up to 25th June 2020, the State of São Paulo had 248,587 confirmed cases with 13,759 deaths.

One important question is related to the patient's immunity after recovery. The difference in immunity after recovery have been reported in humans in [12], and in experiments with rhesus macaques [13]. The experiment in [12] collected plasma from 175 Covid-19 recovered patients, and SARS-CoV-2-specific neutralizing antibodies (NAbs) were detected from day 10 to 15 after the onset of the disease and remained thereafter. Nonetheless, the NAbs levels were variable in the cohort, 52 ( $\approx 30\%$ ) of the patients developed low levels of these antibodies, from which with 10 ( $\approx 6\%$  of the recovered patients) the NAbs levels were undetectable, 25 ( $\approx 14\%$ ) developed high levels.

In [14] the data suggests that the response to SARS-CoV-2 is imbalanced regarding to controlling the virus replication versus the activation of the adaptive immune response. In some cases the immune system doesn't work properly and lung cells remain vulnerable to infection. The virus continues replicating while the immune response system attacks infected cells, killing even healthy nearby cells, and the lung tissue becomes seriously inflamed. This seems to be the mechanism that make some patients become severely ill weeks after their initial infection. Additionally, SARS-CoV-2 probably induces immunity like other coronaviruses, however, it is so new that this mechanism isn't fully understood [15].

The economic crisis due to the pandemics is another important issue. According to [16] the mortality rate of Covid-19 is not necessarily correlated with the economic risk to global economy since governments, companies, consumers and media reacted to the economic shock. However, a global recession seems to be inevitable, its duration and intensity will depend on the success of measures to prevent the spread of Covid-19.

Taking the whole scenario into account researchers worldwide are intensively studying and developing mathematical models of the Covid-19 outbreak. The knowledge on this pandemic dynamics is important for providing estimates on the duration and peaks of the outbreak.

The macro-modelling of infectious disease spread have been a field of research from many years since the simple deterministic model of Kermack and McKendrick [17, 18, 19, 20], that provides a dynamical model classifying individuals in a population as Susceptible - Infected - Removed (SIR) [21]. A number of classical models such as SIR [22] and Susceptible - Exposed - Infected - Removed (SEIR) [23, 24] have been proposed for epidemic modelling.

In addition, works considering time delayed [25] and fractional order [26] dynamical systems applied to Covid-19 outbreak have also been proposed.

In [27] a SIRD model had been adjusted to Covid-19 spreads in China, Italy and France. The results have shown that the recovery rate were similar for the situations of China, Italy and France. In [28], a mixed analytical-statistical inverse problem is used to predict the Covid-29 progression in Brazil, a SIRU model, where U stands for Unreported cases, was used for the direct problem, and a mixture of parameter estimation with Bayesian inference for the inverse problem analysis.

Compartmental models considering immigration and home isolation, or quarantine, are proposed on [10], all the situations presented infection-endemic equilibrium, the results demonstrated that home isolation, or lockdown, mitigates the chance of infection.

In this work the proposed model is a modification of the original compartmental SIR model of Kermack and McKendrick [17, 18, 19], including a sick ( $S_{ick}$ ) population compartment representing nodes of the network that manifest the symptoms of the disease. The proposed Susceptible - Infected - Removed - Sick (SIRSi) model also considers the birth and death of individuals in the given population. In addition, a feedback from those recovered who did not gain immunity or loss their immunity after a period of time and become susceptible again is also introduced.

The proposed SIRSi model presents both a disease free and an endemic equilibrium, and the influence of the re-susceptibility feedback is investigated both analytically and numerically.

The parameters of the proposed SIRSi model are numerically fitted to the

epidemic situation for three cities of the São Paulo State, Brazil, namely, São Paulo, the capital of the State; Santos, on the coast and approximately 80 Km away from São Paulo; and Campinas, in the interior of the state and approximately 90 Km distant from the capital São Paulo, providing estimates for diagnosis and forecasting of the Covid-19 epidemics spread.

The paper is organized as follows, on section 2 the SIRSi compartmental mathematical model is presented. The equilibrium points existence and stability conditions are discussed in section 3, showing the possibility of both endemic and disease-free equilibrium. The parameter fitting of the SIRSi model for the cities of São Paulo, Santos and Campinas is shown in section 4, and the numerical experiments results in section 5. The concluding remarks can be seen in section 6.

## 2. A modified SIR model with birth and death cases

The proposed SIRSi model can be seen in Fig. 1. In this model, the susceptible population  $S$  is infected at a rate  $\alpha$  when contact infected individuals from  $I$ . The susceptible compartment also receives a population, at a rate  $1/\gamma$ , who didn't gain complete immunity after recovering or who loss their immunity after a period of time.

The compartment  $I$  represents the infectious population in incubation stage prior the onset of symptoms. Infection transmission during this period has been reported in [29, 30, 31, 32]. The infected population can be asymptomatic or symptomatic. The period between infection and onset of symptoms,  $1/\beta_2$ , ranges from 3 to 38 days with median of 5.2. Once the infected individual is tested positive and the case is documented, the case is moved to the  $S_{ick}$  compartment. Those who don't develop severe symptoms become asymptomatic.

In [33] the estimative of the infections originated from undocumented cases is as high as 86%, which include mild, limited and lack of symptoms infectious individuals. In other recent studies [34, 35], it was found that, 20% - 40% of positive tested patients were asymptomatic.

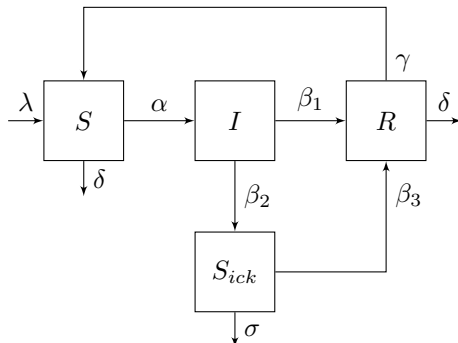


Figure 1: Epidemiological SIRSi model.

In this work, and according to [36], the asymptomatic population is considered as those of under-reporting cases. This population could be as 7 times bigger than the size of the documented cases. This group, under-reporting cases, become recovered with the period  $1/\beta_1$ .

Some of the individuals within this population could eventually develop symptoms. In [37], it has been reported that the average time between infection and the onset of symptoms can be 4.6 days. Once the case becomes documented it should be moved to the  $S_{ick}$  compartment.  $S_{ick}$  are those infected which seek for medical attention with severe symptoms. This population are those who tested positive for COVID-19. In [38] it was reported that this population could represent up to 19.9% of the total documented cases, of which 13.8% are severe cases and 6.1% require intensive care. The sick population become recovered with the period  $1/\beta_3$  or removed at a rate  $\sigma$  (see Fig. 1).

In order to consider the social distancing measure effect in the number of infected and deaths toll shown in Fig. 1, the parameter  $\theta$  is introduced on the mathematical model (1), where  $\theta$  is subject to the constraint  $0 < \theta < 1$ . Consequently, given these facts, the mathematical SIRSi model is given by (1),

$$\begin{aligned}
\dot{S} &= \lambda - \alpha(1 - \theta)SI - \delta S + \gamma R, \\
\dot{I} &= \alpha(1 - \theta)SI - (\beta_1 + \beta_2)I, \\
\dot{S}_{ick} &= \beta_2 I - (\beta_3 + \sigma)S_{ick} \\
\dot{R} &= \beta_1 I + \beta_3 S_{ick} - (\gamma + \delta)R
\end{aligned} \tag{1}$$

where  $\lambda$  and  $\delta$  are the birth and death rates, respectively.

It is important to notice that the number of documented cases is a key information that should emerge, somehow, from (1). The reason is the fact that the accumulated number of confirmed cases is publicly available, and will be used to fine-tuning the model. The number of daily new infections is also available, but it tends to be noisy and less representative of the dynamics.

### 3. Disease-free and endemic equilibrium points

Considering (1), such that  $\dot{x} = f(x)$ , where  $x = (S, I, S_{ick}, R)^T$ ,  $x \in \mathbb{U} \subset (\mathbb{R}_0^+)^4$ ,  $f : \mathbb{U} \rightarrow \mathbb{U}$  is the right-hand side of (1), and parameters  $\alpha, \beta_1, \beta_2, \beta_3, \sigma, \gamma, \theta \in \mathbb{R}^+$ .

To investigate the influence of the introduction of the feedback from those recovered with no immunity which become susceptible again, and dividing the population into groups, the equilibrium points related to the model described by (1) must be determined and their stability discussed.

Assuming  $\alpha \neq 0$ , i.e., susceptible can be converted into infected, and despite being an assumption it is realistic for a spreading disease, the equilibrium points are such that  $f(x^*) = 0$ .

Using the Hartman-Grobman Theorem [39] the local stability of the equilibrium points can be determined by the eigenvalues of the Jacobian matrix computed on each equilibrium point. The Jacobian  $J = \frac{\partial f}{\partial x} \Big|_{x^*}$  of (1) is given by (2).

$$J = \begin{bmatrix} -(\delta + I^* \alpha(1 - \theta)) & -S^* \alpha(1 - \theta) & 0 & \gamma \\ I^* \alpha(1 - \theta) & S^* \alpha(1 - \theta) - (\beta_2 + \beta_1) & 0 & 0 \\ 0 & \beta_2 & -(\beta_3 + \sigma) & 0 \\ 0 & \beta_1 & \beta_3 & -(\delta + \gamma) \end{bmatrix} \quad (2)$$

In the following the disease-free (section 3.1) and the endemic (section 3.2) equilibrium points are determined.

### 3.1. Disease-free equilibrium points

The disease-free equilibrium is a state corresponding to the absence of infected individuals, *i.e.*,  $I^* = 0$ . Applying this condition to the equilibrium of (1), the point can be determined.

Assume that there exist a disease free-equilibrium ( $I^* = 0$ ),  $x^* \in \mathbb{U}$ , such that  $f(x^*) = 0$ . This equilibrium point  $x^* = (S^*, I^*, S_{ick}^*, R^*)^T$  with  $x^*$  in the first octant of  $\mathbb{R}^4$  is given by:

$$P_1 = (S^*, I^*, S_{ick}^*, R^*)^T = (\lambda/\delta, 0, 0, 0)^T. \quad (3)$$

Considering  $P_1$ , the corresponding linear system Jacobian [39]  $J_{P_1} = \frac{\partial f}{\partial x} \Big|_{x^*}$  is given by (4).

$$J_{P_1} = \begin{bmatrix} -\delta & -\alpha(1 - \theta)(\lambda/\delta) & 0 & \gamma \\ 0 & \alpha(1 - \theta)(\lambda/\delta) - (\beta_1 + \beta_2) & 0 & 0 \\ 0 & \beta_2 & -(\beta_3 + \sigma) & 0 \\ 0 & \beta_1 & \beta_3 & -(\delta + \gamma) \end{bmatrix}. \quad (4)$$

By the Laplace determinant development [40], the eigenvalues of (4) are the elements in the diagonal, that is,  $\xi_1 = -\delta$ ,  $\xi_2 = \alpha(1 - \theta)(\lambda/\delta) - (\beta_1 + \beta_2)$ ,  $\xi_3 = -(\beta_3 + \sigma)$  and  $\xi_4 = -(\delta + \gamma)$ .

The eigenvalues above with the Hartman-Grobman Theorem indicates that (1) presents one disease-free equilibrium point, and considering the condition



given by the eigenvalue  $\xi_2 = \alpha(1 - \theta)\lambda/\delta - (\beta_1 + \beta_2)$ , if  $\alpha(1 - \theta)\lambda/\delta < (\beta_1 + \beta_2)$  the eigenvector associated indicates an asymptotically stable direction. Consequently, if  $\alpha(1 - \theta)\lambda/\delta > (\beta_1 + \beta_2)$  the equilibrium point  $P_1$  is unstable, indicating a bifurcation in the parameter space.

### 3.2. Endemic equilibrium points

The endemic equilibrium points are characterized by the existence of infected people in the population, that is,  $(I^* \neq 0)$ .

Therefore, assuming the existence of an endemic equilibrium point, with  $x^* \in \mathbb{U}$ , such that  $f(x^*) = 0$ , the equilibrium point  $P_2 = x^* = (S^*, I^*, R^*, S_{ick}^*)^T$  in the first octant of  $\mathbb{R}^4$  is given by (6),

$$\begin{aligned} S^* &= \frac{\beta_1 + \beta_2}{\alpha(1 - \theta)} \\ I^* &= \frac{1}{\phi} (\delta + \gamma) (\beta_3 + \sigma) [\alpha(1 - \theta)\lambda - (\beta_1 + \beta_2)\delta] \\ S_{ick}^* &= \frac{1}{\phi} \beta_2 (\delta + \gamma) [\lambda\alpha(1 - \theta) - (\beta_1 + \beta_2)\delta] \\ R^* &= \frac{1}{\phi} (\beta_1\beta_3 + \beta_2\beta_3 + \beta_1\sigma) [\alpha(1 - \theta)\lambda - (\beta_1 + \beta_2)\delta], \end{aligned} \tag{5}$$

where  $\phi = \alpha(1 - \theta) (\beta_1\beta_3\delta + \beta_2\beta_3\delta + \beta_1\delta\sigma + \beta_2\delta\sigma + \beta_2\gamma\sigma)$ .

Accordingly, the existence condition of a positive endemic equilibrium  $P_2 = x^* = (S^*, I^*, R^*, S_{ick}^*)^T \in \mathbb{R}^+$  is given by (6).

$$\alpha(1 - \theta)\frac{\lambda}{\delta} > \beta_1 + \beta_2. \tag{6}$$

Note that condition (6) reflects the fact that, in order to the endemic equilibrium exists, the rate  $\alpha$  at which, the people flux rate, represented by  $\lambda/\delta$ , become infected, has to be greater than the rate at which infected population leave the compartment  $I$ , either overcoming the disease or becoming symptomatic.

It is important to highlight that  $\lambda/\delta$  could also represent the total people flux commuting from a different city in a multi-population model.

The linearization  $A = J_{P_2} = \left. \frac{\partial f}{\partial x} \right|_{x^*}$  at the endemic equilibrium is:

$$A = \begin{bmatrix} -(\delta + I^* \alpha(1 - \theta)) & -(\beta_1 + \beta_2) & 0 & \gamma \\ I^* \alpha(1 - \theta) & 0 & 0 & 0 \\ 0 & \beta_2 & -(\beta_3 + \sigma) & 0 \\ 0 & \beta_1 & \beta_3 & -(\delta + \gamma) \end{bmatrix}. \quad (7)$$

The characteristic polynomial  $\det(A - I_d \xi) = 0$  is

$$\xi^4 + a_1 \xi^3 + a_2 \xi^2 + a_3 \xi + a_4 = 0, \quad (8)$$

with

$$\begin{aligned} a_1 &= \beta_3 + 2\delta + \gamma + \sigma + I^* \alpha(1 - \theta); \\ a_2 &= I^* \alpha(1 - \theta) (\beta_1 + \beta_2 + \beta_3 + \delta + \gamma + \sigma) + 2\delta(\beta_3 + \sigma) + \\ &\quad \gamma(\beta_3 + \delta + \sigma) + \delta^2; \\ a_3 &= I^* \alpha(1 - \theta) [\beta_1 \beta_3 + \beta_2 \beta_3 + (\beta_1 + \beta_2 + \beta_3) \delta + (\beta_2 + \beta_3) \gamma + \\ &\quad (\beta_1 + \beta_2 + \delta + \gamma) \sigma] + \beta_3 \delta^2 + \delta^2 \sigma + \beta_3 \delta \gamma + \delta \gamma \sigma; \\ a_4 &= I^* \alpha(1 - \theta) (\beta_1 \beta_3 \delta + \beta_2 \beta_3 \delta + \beta_1 \delta \sigma + \beta_2 \delta \sigma + \beta_2 \gamma \sigma). \end{aligned} \quad (9)$$

Any further effort to analytically analyze  $\xi$  eigenvalues, becomes quite difficult due to the coefficients complexity. A possible alternative approach is to go for numerical calculations.

However, some insight for the model with feedback  $\gamma$  can be obtained, in terms of bifurcations and stability, if we analyze the eigenvalues when  $\gamma = 0$  and  $\gamma \neq 0$ .

### 3.2.1. Eigenvalues for $\gamma = 0$

Note that in this case, the endemic equilibrium is still possible. Computing the eigenvalues results,

$$\begin{aligned}
\xi_1 &= -\delta, \\
\xi_2 &= -(\beta_3 + \sigma), \\
\xi_3 &= \frac{1}{2(\beta_1 + \beta_2)}(-\alpha(1 - \theta)\lambda + \sqrt{\Delta}), \\
\xi_4 &= \frac{1}{2(\beta_1 + \beta_2)}(-\alpha(1 - \theta)\lambda - \sqrt{\Delta}),
\end{aligned} \tag{10}$$

such that  $\Delta = 4\delta(\beta_1 + \beta_2)^3 + (\alpha(1 - \theta))^2\lambda^2 - 4\lambda\alpha(1 - \theta)(\beta_1 + \beta_2)^2$ .

The eigenvalues  $\xi_3$  and  $\xi_4$  can be either complex conjugate stable, or both real. The eigenvalue  $\xi_3$  needs to be further studied due to the possibility of bifurcation.

Analysing the eigenvalue  $\xi_3$ , if  $\alpha(1 - \theta)\lambda > \sqrt{\Delta}$ ,  $P_2$  is stable, and consequently (6) holds true.

On the other hand, if  $\alpha(1 - \theta)\lambda < \sqrt{\Delta}$ , the endemic equilibrium point is unstable, and the existence condition (6) is not satisfied, consequently, the endemic equilibrium point  $P_2$ , if existing, is stable.

### 3.2.2. Eigenvalues for $\gamma \rightarrow \infty$

Another insight can be obtained by looking with the case  $\gamma \rightarrow \infty$ . In this case, the endemic equilibrium becomes:

$$\begin{aligned}
S^* &= \frac{\beta_1 + \beta_2}{\alpha(1 - \theta)}, \\
I^* &\rightarrow \frac{(\beta_3 + \sigma)}{\alpha(1 - \theta)\beta_2\sigma} [\alpha(1 - \theta)\lambda - (\beta_1 + \beta_2)\delta] \\
S_{ick}^* &\rightarrow \frac{\beta_1 + \beta_2}{\alpha(1 - \theta)}, \\
R^* &\rightarrow 0,
\end{aligned} \tag{11}$$

which is subject to the same existence condition given in equation (6).

Under the assumption  $\gamma \rightarrow \infty$ , the characteristic polynomials coefficients in equation (9) can be approximated by (12):

$$\begin{aligned}
a_1 &\approx \gamma, \\
a_2 &\approx \gamma(I^* \alpha(1 - \theta) + \beta_3 + \delta + \sigma) = \gamma b_2, \\
a_3 &\approx \gamma(I^* \alpha(1 - \theta) (\beta_2 + \beta_3 + \sigma) + \delta(\beta_3 + \sigma)) = \gamma b_3, \\
a_4 &= \gamma I^* \alpha(1 - \theta) \beta_2 \sigma = \gamma b_4,
\end{aligned} \tag{12}$$

the characteristic polynomial (8) can be rewritten as in (13):

$$\begin{aligned}
\xi^4 + \gamma\xi^3 + \gamma b_2 \xi^2 + \gamma b_3 \xi + \gamma b_4 &= 0, \\
\xi^4 + \gamma(\xi^3 + b_2 \xi^2 + b_3 \xi + b_4) &= 0,
\end{aligned} \tag{13}$$

assuming that at least one root  $|\xi|$  goes to infinity as  $\gamma \rightarrow \infty$ , we rewrite the polynomial as

$$\begin{aligned}
\xi^4 + \gamma\xi^3 &= 0, \\
\xi^3(\xi + \gamma) &= 0,
\end{aligned} \tag{14}$$

then,

$$\xi_1 = -\gamma, \text{ and } \gamma \rightarrow \infty,$$

so, one eigenvalue seem to be going to  $-\infty$  as  $\gamma \rightarrow \infty$ . To find an approximation to the other three roots, the characteristic polynomial is rewritten in equation (13). It can be also assumed that the other three roots are finite,

$$\begin{aligned}
\xi^4 + \gamma\xi^3 + \gamma b_2 \xi^2 + \gamma b_3 \xi + \gamma b_4 &= 0, \\
\frac{1}{\gamma} \xi^4 + \xi^3 + b_2 \xi^2 + b_3 \xi + b_4 &= 0, \\
&\approx \xi^3 + b_2 \xi^2 + b_3 \xi + b_4 = 0.
\end{aligned} \tag{15}$$

Looking for insight numerical experiments are performed.

#### 4. Parameters fitting by the least-squares method

In this section the parameters of the proposed SIRSi model (1) (see Fig. 1) are numerically adjusted to fit the curve for confirmed symptomatic infected

cases of three major cities in the state of São Paulo - Brazil, using public available data from the State Data Analysis System - SEADE (*Sistema Estadual de Análise de Dados*<sup>2</sup>). The total population for the cities was obtained from the same source and it is shown in table 1.

City	Total population in 2020
São Paulo	11.869.660
Campinas	1.175.501
Santos	428.703

Table 1: Total population collected from SEADE.

To calculate birth and death rates,  $\lambda$  and  $\delta$  respectively, linear interpolation was necessary, as the data from the public repository was out of date, results are shown in Fig. 2.

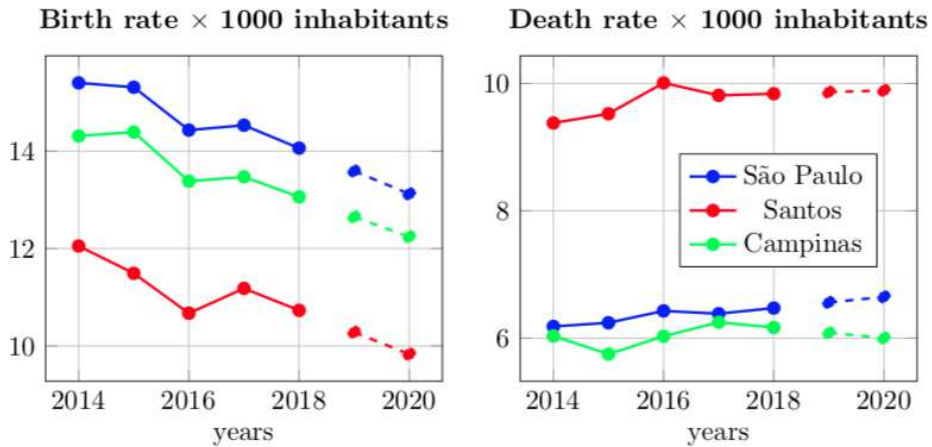


Figure 2: Birth and death rates per 1000 inhabitants for São Paulo, Santos and Campinas. Public data is shown in solid lines and interpolated values are shown in dashed lines.

One of the first actions against the spread of the virus was the imposition of a social distancing measure which was first decreed in São Paulo on May 17. This intervention, represented by  $\theta$  in the model, focuses on reducing the

<sup>2</sup><https://www.seade.gov.br/>

possible contact between infected and susceptible individuals, so it is introduced as a factor of the transmission rate, i.e.  $\alpha(1 - \theta)$ . The time series corresponding to the daily measures of this index along with their mean for each one of the cities considered are shown in figure 3. Although this time variation resembles a 7-day periodic function, especially on the second half of the register, we use as a first approximation the mean of this measure as a representative value.

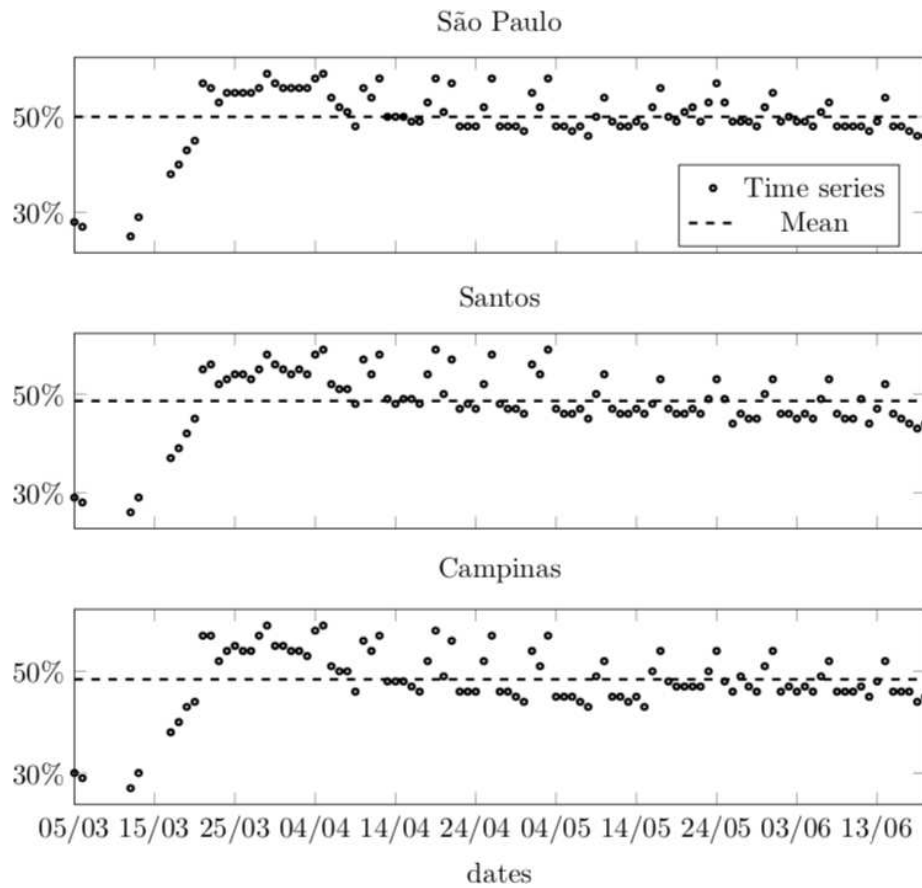


Figure 3: Percentage of social distancing [41].

By the time we write, there is not much information about the duration of the antibody response to SARS-CoV-2, however what is known so far is that protection after recovery wanes over time. Recent research highlights that immune response and antibodies protection after recovery may depend on the

severity of the infection, in some cases this protection can last for as little as 12 weeks while in others few cases no antibodies protection is obtained at all [42, 43, 44, 45, 46, 47]. To assess the influence of this behavior on the disease spread, we set the feedback parameter  $\gamma$  at constant values  $\gamma \in \{0, 0.01, 0.02, 0.03, 0.04\}$  in order to map possible scenarios especially those related to possible second waves of infection.

The transmission rate of symptomatic individuals prior hospitalization is estimated between 1.12 to 1.19 while for asymptomatic cases this rate ranges between 0.1 to 0.6, in model (1) this parameter is represented by the product  $\alpha(1-\theta)$ , thus, we let  $\alpha \in [0.1, 1.0]$ . The mean time between infection and onset-of-symptoms for confirmed cases,  $1/\beta_2$ , is 2 days, thus we let  $\beta_2 \in [0.1, 0.6]$ . The time from onset-of-infection to fully recovery,  $1/\beta_1$ , is considered to be between a few days up to two weeks (5 to 15 days). The period of time it takes for a symptomatic patient to overcome the disease,  $1/\beta_3$ , and the time between hospitalization to death,  $1/\sigma$ , are both considered to be between 5 to 20 days [48, 37, 38, 49].

The trust-region reflective least-squares algorithm [50, 51, 52] along with a 4th-order Runge-Kutta integrator were used to fit parameters in model (1) to actual data collected from public repositories for each one of the three cities into consideration. All parameters and initial conditions computed are normalized with respect to the total population in each case. For the fitting, we set  $S_0 \in [0, 1]$ ,  $I_0 \in [0, 1]$  with initial guess  $S_0^i = 99.9\%$  and  $I_0^i = 0.1\%$ , the initial condition for  $S_{ick}$  and  $R$  was set to zero. Results are shown in tables 2 to 7, and the temporal evolution of the  $S_{ick}$  compartment for each city, for both, the fitted model and the public data, is show in figures 6, 8 and 10.

In order to assess the influence of the parameter  $\gamma$  in the endemic equilibrium, the eigenvalues were plotted for the set of fitted parameters found, for  $\gamma \in [0, 2)$ . In figures 4 are shown the eigenvalues for the endemic equilibrium for each city computed for each one of the fitted sets. At  $\gamma = 0$  eigenvalues are stable for São Paulo e Santos, as  $\gamma$  increases, eigenvalues move towards the left-hand side of the complex plane, whereas for Campinas eigenvalues are unstable for  $\gamma = 0$ .

	<b>Fit 1</b>	<b>Fit 2</b>	<b>Fit 3</b>	<b>Fit 4</b>	<b>Fit 5</b>
$\alpha$	9.377e-01	9.512e-01	9.312e-01	9.484e-01	8.485e-01
$\beta_1$	1.181e-01	1.553e-01	1.881e-01	1.991e-01	1.999e-01
$\beta_2$	2.978e-01	2.646e-01	2.179e-01	2.145e-01	1.698e-01
$\beta_3$	6.325e-02	8.144e-02	1.248e-01	1.396e-01	1.661e-01
$\sigma$	1.117e-01	8.837e-02	7.195e-02	6.271e-02	5.830e-02
$\lambda$	3.595e-05	3.595e-05	3.595e-05	3.595e-05	3.595e-05
$\delta$	1.822e-05	1.822e-05	1.822e-05	1.822e-05	1.822e-05
$\theta$	5.005e-01	5.005e-01	5.005e-01	5.005e-01	5.005e-01
$\gamma$	0.000e+00	1.000e-02	2.000e-02	3.000e-02	4.000e-02

Table 2: Fitted parameter for São Paulo.

	<b>Fit 1</b>	<b>Fit 2</b>	<b>Fit 3</b>	<b>Fit 4</b>	<b>Fit 5</b>
$S_0$	9.940e-01	9.888e-01	9.857e-01	9.827e-01	9.961e-01
$I_0$	4.319e-05	4.758e-05	5.340e-05	5.773e-05	7.675e-05
$S_{ick0}$	8.425e-08	8.425e-08	8.425e-08	8.425e-08	8.425e-08
$R_0$	0.000e+00	0.000e+00	0.000e+00	0.000e+00	0.000e+00

Table 3: Fitted initial conditions for São Paulo.

	<b>Fit 1</b>	<b>Fit 2</b>	<b>Fit 3</b>	<b>Fit 4</b>	<b>Fit 5</b>
$\alpha$	9.131e-01	9.479e-01	9.835e-01	7.840e-01	9.355e-01
$\beta_1$	1.600e-01	1.884e-01	1.932e-01	1.652e-01	1.929e-01
$\beta_2$	2.440e-01	2.261e-01	2.459e-01	1.760e-01	2.024e-01
$\beta_3$	5.070e-02	7.930e-02	1.112e-01	9.574e-02	1.469e-01
$\sigma$	7.973e-02	5.095e-02	2.750e-02	6.898e-02	2.503e-02
$\lambda$	2.693e-05	2.693e-05	2.693e-05	2.693e-05	2.693e-05
$\delta$	2.710e-05	2.710e-05	2.710e-05	2.710e-05	2.710e-05
$\theta$	4.860e-01	4.860e-01	4.860e-01	4.860e-01	4.860e-01
$\gamma$	0.000e+00	1.000e-02	2.000e-02	3.000e-02	4.000e-02

Table 4: Fitted parameter for Santos.

In 5 a closer view of the eigenvalues around the origin are shown.



	<b>Fit 1</b>	<b>Fit 2</b>	<b>Fit 3</b>	<b>Fit 4</b>	<b>Fit 5</b>
$S_0$	1.006e+00	9.927e-01	1.004e+00	1.017e+00	9.685e-01
$I_0$	1.141e-05	1.141e-05	1.168e-05	1.852e-05	1.402e-05
$S_{icks0}$	0.000e+00	0.000e+00	0.000e+00	0.000e+00	0.000e+00
$R_0$	0.000e+00	0.000e+00	0.000e+00	0.000e+00	0.000e+00

Table 5: Fitted initial conditions for Santos.

	<b>Fit 1</b>	<b>Fit 2</b>	<b>Fit 3</b>	<b>Fit 4</b>	<b>Fit 5</b>
$\alpha$	7.473e-01	7.472e-01	7.466e-01	7.464e-01	7.384e-01
$\beta_1$	1.350e-01	1.352e-01	1.354e-01	1.355e-01	1.368e-01
$\beta_2$	1.930e-01	1.934e-01	1.933e-01	1.934e-01	1.923e-01
$\beta_3$	5.631e-02	5.582e-02	5.225e-02	5.281e-02	5.965e-02
$\sigma$	1.995e-01	1.954e-01	1.899e-01	1.906e-01	1.996e-01
$\lambda$	3.353e-05	3.353e-05	3.353e-05	3.353e-05	3.353e-05
$\delta$	4.509e-05	4.509e-05	4.509e-05	4.509e-05	4.509e-05
$\theta$	4.842e-01	4.842e-01	4.842e-01	4.842e-01	4.842e-01
$\gamma$	0.000e+00	1.000e-02	2.000e-02	3.000e-02	4.000e-02

Table 6: Fitted parameter for Campinas.

	<b>Fit 1</b>	<b>Fit 2</b>	<b>Fit 3</b>	<b>Fit 4</b>	<b>Fit 5</b>
$S_0$	1.008e+00	1.008e+00	1.007e+00	1.007e+00	1.005e+00
$I_0$	8.749e-06	9.148e-06	9.364e-06	9.614e-06	1.776e-05
$S_{icks0}$	0.000e+00	0.000e+00	0.000e+00	0.000e+00	0.000e+00
$R_0$	0.000e+00	0.000e+00	0.000e+00	0.000e+00	0.000e+00

Table 7: Fitted initial conditions for Campinas.

## 5. Numerical experiments

In this section the numerical experiments are conducted using the MATLAB-Simulink [53] for two different conditions. Firstly, the SIRSi model is fitted with the real data for the  $S_{icks}$  population, and for different values of the parameter  $\gamma$ . In the sequence, the simulation for the infected population  $I$ , that can be inferred from the proposed model, is carried out.

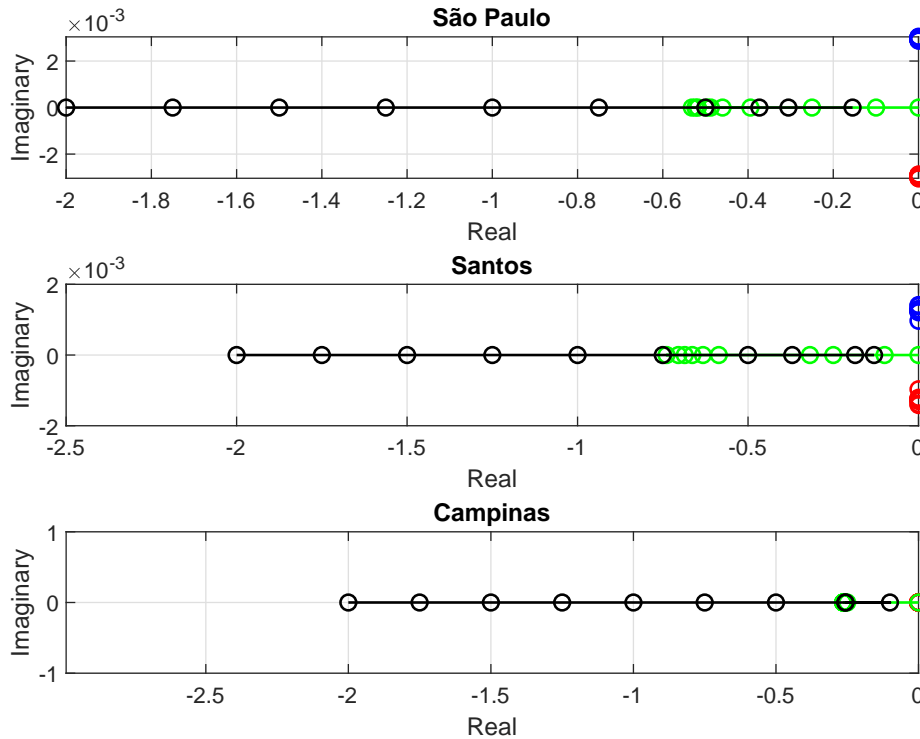


Figure 4: Eigenvalues for  $\gamma \in \{0, 0.1\}$ , for the three cities into consideration.

The numerical experiments, as in section 4, were conducted for three major cities in the state of São Paulo, namely, São Paulo, Campinas, and Santos.

The initial condition is  $x_0 = (S_0, I_0, S_{ick0}, R_0)^T$ , where  $S_0$  and  $I_0$  are the normalized susceptible and infected populations, which are considered free parameters in the sense that they can be modified by the fitting algorithm.

### 5.1. Simulation results for São Paulo

In Fig.6 it can be seen that the SIRSi model is adjusted for the confirmed cases of infected people data.

Considering that the acquired immunity is permanent, *i.e.*,  $\gamma = 0$ , and that the isolation rate is constant, the peak of the infection occurs soon after July 2020, and until the end of the the same year, the disease will not persist, since the number of confirmed cases will go down to zero.

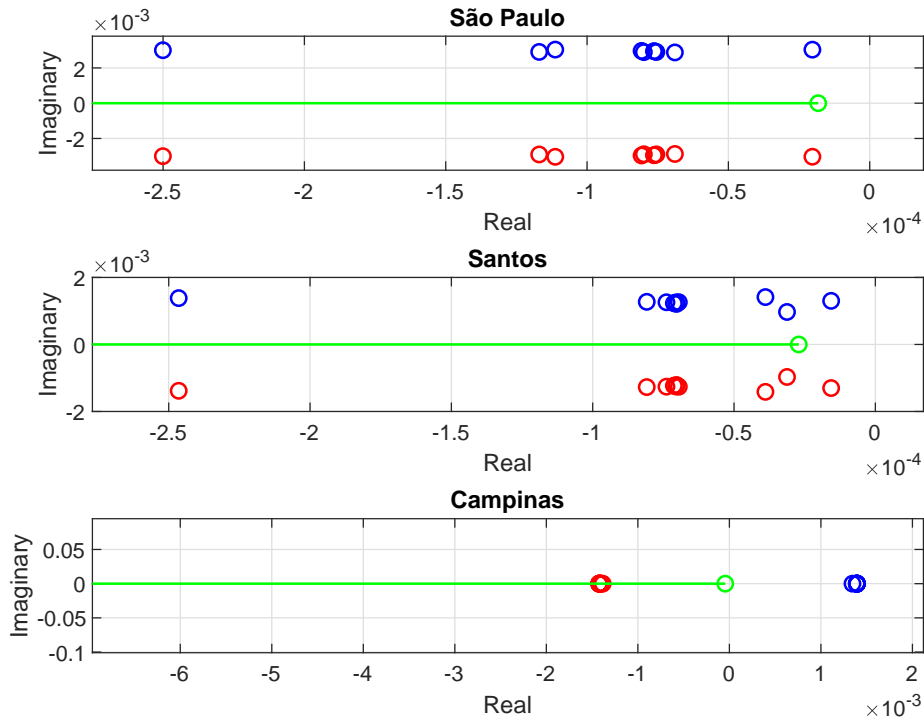


Figure 5: Eigenvalues for  $\gamma \in \{0, 0.1\}$ , closer view around the origin.

On the other hand, assuming that immunity is not permanent and adopting a reinfection rate  $\gamma = 0.01$ , meaning that every 100 days a recovered person becomes susceptible again, the model predicts a decrease in the confirmed cases and a new wave of infection in the first half of 2022.

Decreasing the time interval to 50 days in which a recovered person becomes susceptible ( $\gamma = 0.02$ ), the model indicates a second wave of infection in the first half of 2021. For the situation in which a recovered system is susceptible to each 25 days ( $\gamma = 0.04$ ), the model simulation shows that by the end of this year the number of confirmed infected will reduce by almost two thirds and that the number of infected will continue decreasing over time, but the number of confirmed cases will remain higher than the other simulated curves.

In Fig.7, the infected compartment  $I$  inferred from the SIRS<sub>i</sub> model is presented, showing that the peak of infection is close to July 2020.

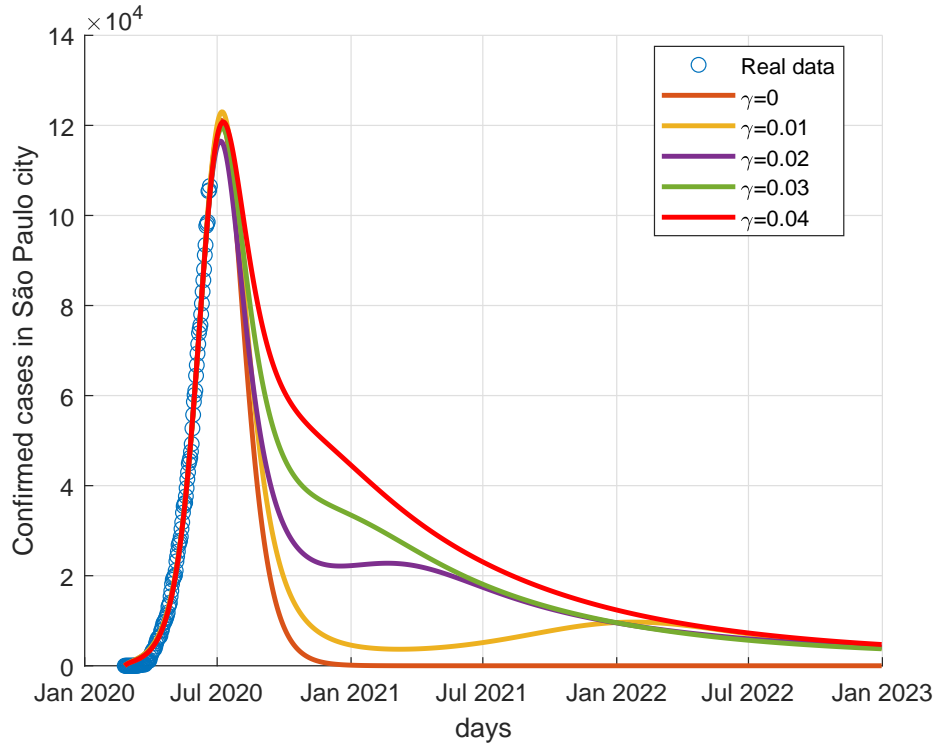


Figure 6: Time evolution for confirmed cases ( $S_{ick}$  population) in São Paulo.

Increasing  $\gamma$  will reduce the time for a recovered person to become susceptible again, causing the peaks in Fig. 7 to increase, when compared to the curves for lower values of  $\gamma$ . This behavior, however, cannot be observed in Fig.6, indicating that the increase the re-susceptibility feedback gain  $\gamma$  possibly contributes to the increase of asymptomatic or unreported infected cases.

In addition, it appears that if those recovered acquire permanent immunity  $\gamma = 0$ , the number of infected people tends to zero by the end of 2020. For  $\gamma = 0.01$ , it appears that there is a small increase in January 2022. For  $\gamma = 0.02$  a new wave of confirmed cases can be seen in Fig.6, and accordingly, the increase in the infected population is also observed in Fig.7.

For São Paulo, the numerical experiments show that considering any reinfection rate, there will be confirmed infected cases and unreported infected cases

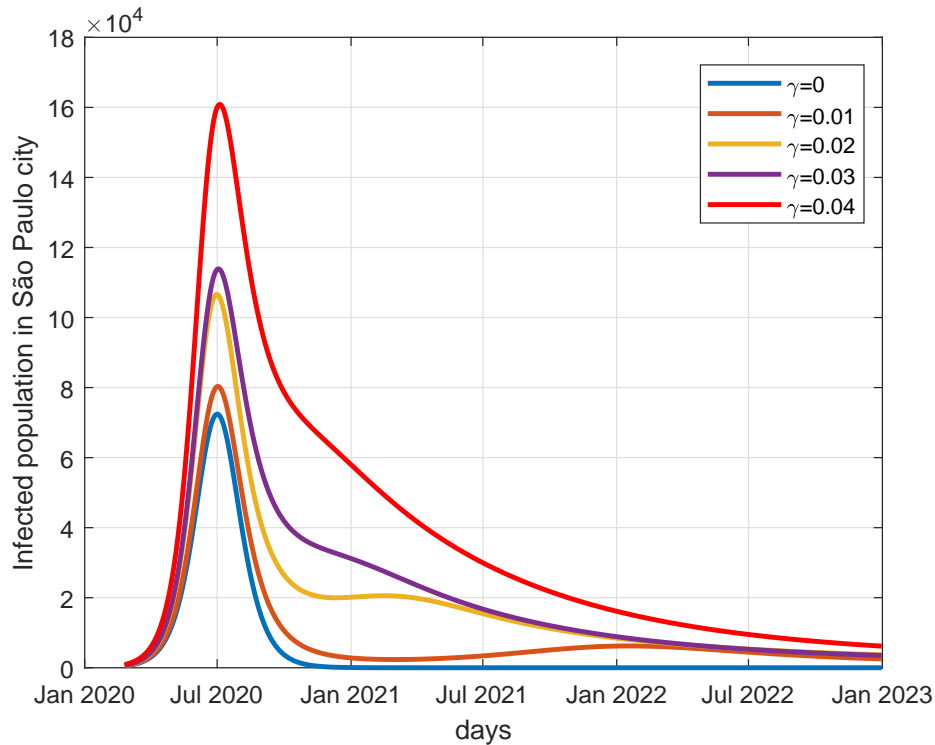


Figure 7: Time evolution for infected population in São Paulo.

until 2023, indicating the need for a control strategy, being necessary and the study of preventive inoculation.

### 5.2. Simulation results for Santos

Fig.8 shows the SIRSi model adjusted to the confirmed cases of infected people data for Santos. Assuming that the immunity acquired is permanent,  $\gamma = 0$ , and that the isolation rate is constant, the peak of the confirmed cases in Santos will occur very close to July 2020. and similarly to São Paulo (see Fig. 6), until the end of the same year, the disease will not persist with the number of confirmed cases going down to zero.

Adopting a nonzero reinfection rate, such that one person every 100 days becomes susceptible again ( $\gamma = 0.01$ ), a second wave of infection is seen in the coastal city around July 2021, one year before the second wave predicted for

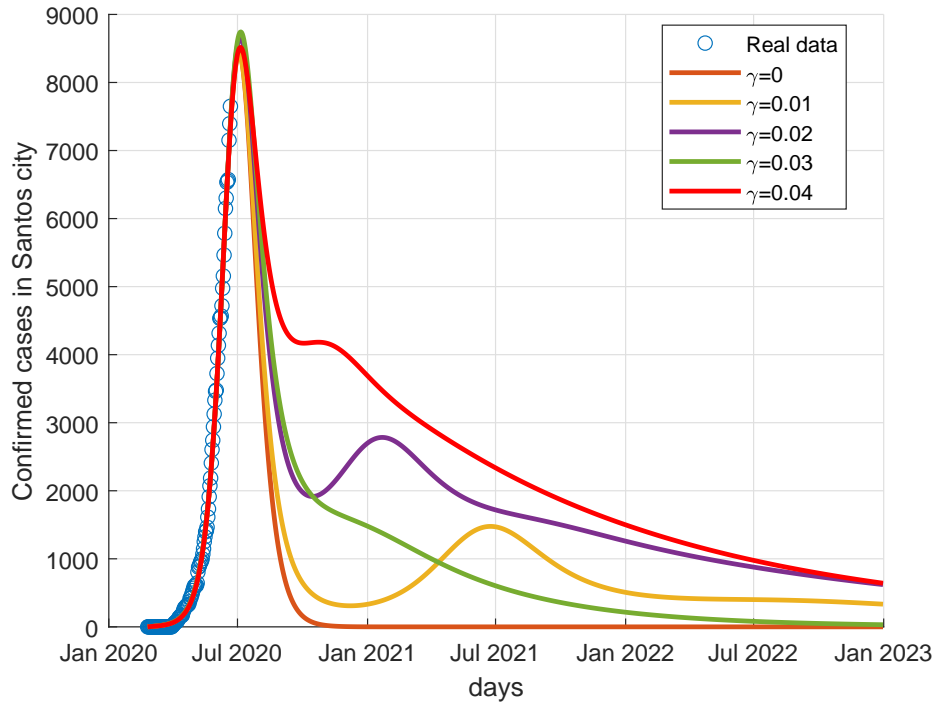


Figure 8: Time evolution for confirmed cases (sick population) in Santos.

São Paulo with the same value for the re-susceptibility feedback gain  $\gamma$ .

Considering  $\gamma = 0.02$ , for which an infected person becomes susceptible again in a time interval of 50 days, the second wave of confirmed cases occurs at the beginning of the first half of 2021 and the number of confirmed infected is reduced to one third of the peak value.

These situations should be analyzed with caution and it is suggested to study the influence of the flow of people between these cities, since in the city of Santos the second waves of infections occur before the city of São Paulo.

For  $\gamma = 0.04$ , after the peak of the confirmed cases, a second wave can be observed in the numerical results before the end of 2020, delaying the reduction of the confirmed cases.

For Santos, the numerical experiments show that for  $\gamma = 0$  and for  $\gamma = 0.03$ , the numbers of confirmed cases tend to zero in the beginning of 2023.

The infected compartment  $I$  inferred from the SIRSi model is presented in Fig. 9, showing that the peak of infection is close to July 2020.

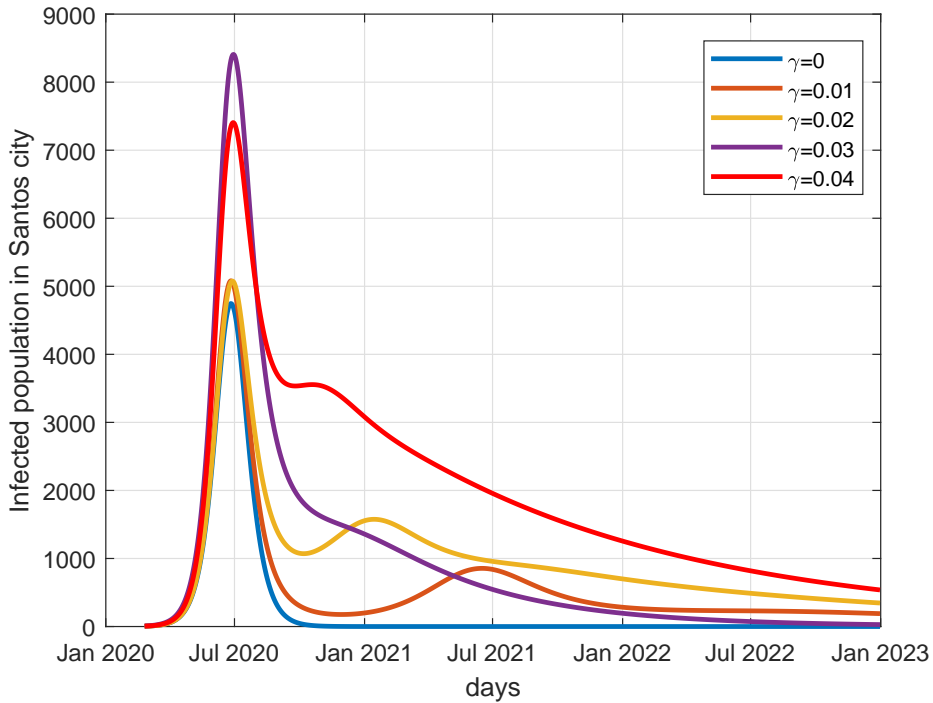


Figure 9: Time evolution for infected population in Santos.

The increase in re-susceptibility feedback gain  $\gamma$ , will reduction the time for an infected person to be susceptible again, causing higher peaks when compared with the curves for lower values of  $\gamma$ . This behavior does not occur in Fig.8 indicating that the increase in feedback possibly contributes to the increase in asymptomatic or unreported infected cases. This situation is similar to what is observed for São Paulo.

In addition, for  $\gamma = 0$ , the number of the infected people  $I$  tends to zero before the end of the 2020 (see the curve for  $\gamma = 0$  in Fig.9).

For  $\gamma = 0.01$ , a new wave of infection in 2021 can be seen, and for  $\gamma = 0.02$  the peak of the second wave of infection is near January 2021 (see Fig.9,  $\gamma = 0.01$  and  $\gamma = 0.02$ ).

Unlike São Paulo, the highest peak of infection among the unreported occurs when  $\gamma = 0.03$  and this behavior suggests a more detailed study of the dynamics, because together with the situation in which the infected person acquires permanent immunity, these rates suggest that the saving of confirmed cases (see Fig.8 and asymptomatic infected individuals tends to zero more quickly.

In the situation in which a recovered person is liable to a new susceptibility in 25 days, it is observed that the infection persists in the population for a longer time, as shown by the curve with  $\gamma = 0.04$  in Fig.9 and justifies the policy strategies public policies, including vaccination.

### 5.3. Simulation results for Campinas

In Fig. 10 the SIRSi model adjusted to the confirmed cases of infected people data in Campinas is shown.

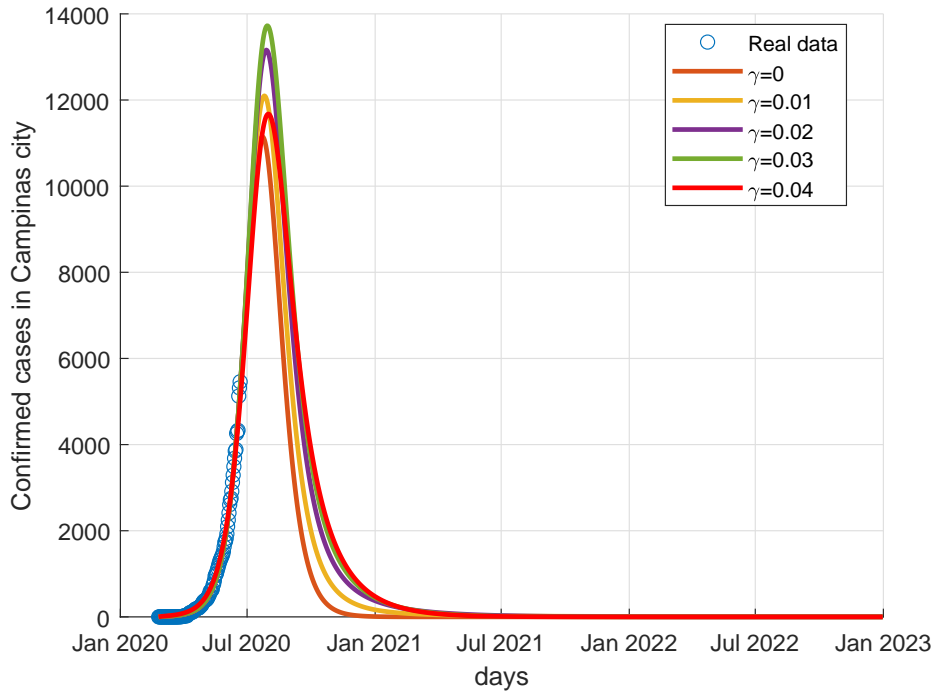


Figure 10: Time evolution for confirmed cases (sick population) in Campinas.

For permanent acquired immunity,  $\gamma = 0$ , and constant isolation rate, the



peak of confirmed infection cases occur in the beginning of the second half of 2020.

Considering the re-susceptibility feedback gain  $\gamma > 0$ , in Fig. 10, it seems that with the increasing of  $\gamma$  the time necessary for the number of confirmed infected cases go down to zero is slightly bigger, unlike the other two cities studied. In addition, Campinas does not present a second wave of infection, even with the variation  $\gamma$ .

The general behavior of Campinas, concerning the sensitivity analysis for  $\gamma$ , present results that differ from Santos and São Paulo. It can be noticed in Fig. 10 that the observed data are far from the peak of infection predicted by the SIRSi model. At this point, more data is needed for any further qualitative analysis.

Observing the eigenvalues for the city of Campinas (See Figs. 4 and 5) it can be noticed that they are all real, indicating that there is no oscillatory behavior in the dynamics of the model. Depending on the new data this situation might change.

The infected compartment of Campinas presents the peak of infection close to the beginning of the second half of 2020, Fig.11.

The increase in the reinfection parameter, causes the peak to increase and this occurs in the figure Fig.10 indicating that the increase in feedback possibly contributes to the increase in asymptomatic or unreported infected.

## 6. Conclusions

The proposed SIRSi model was fitted to publicly available data of the Covid-19 outbreak, providing estimates on the duration and peaks of the outbreak. In addition, the model allows to infer information related to unreported and asymptomatic cases.

The proposed model with feedback adjusted to the confirmed infection data, suggests the possibility of the recovered ones having temporary immunity  $\gamma > 0$  or even permanent  $\gamma = 0$ .

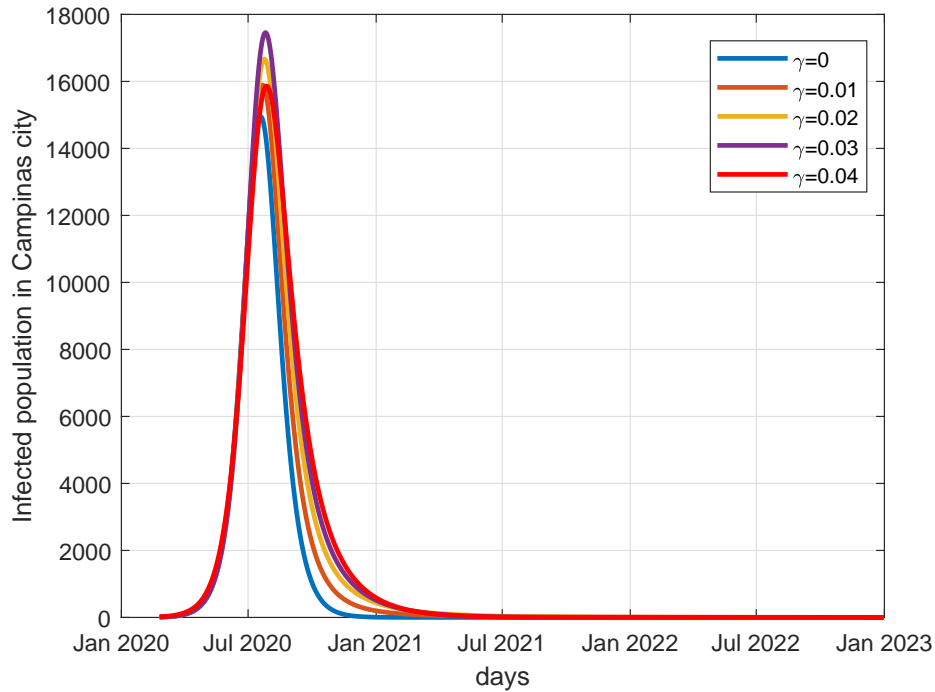


Figure 11: Time evolution for infected population in Campinas.

Considering the situation in which immunity is temporary, there is a second wave of infection which, depending on the time interval for a recovered person to be susceptible again, indicates a second wave with a greater or lesser number of reinfected persons.

If the time interval is shorter (larger  $\gamma$ ), the second wave of infection will have a greater number of infected people when compared to a shorter time interval of the feedback.

The qualitative behavior for São Paulo and Santos are similar in terms the sensitivity analysis of the re-susceptibility feedback gain  $\gamma$ . The bigger the  $\gamma$  the shorter the time for a recovered person to become susceptible again to infection, increasing unreported or asymptomatic cases.

For the city of Campinas, it is suggested to collect more data, because as the data of the confirmed infected presents a certain distance from the peak of the infection, the dynamics of the model may undergo some significant change,

given the sensitivity of the model to disturbances.

## 7. Availability of data and materials

Data are publicly available with [54, 41].

## 8. Declaration of competing interest

There is no conflict of interest between the authors.

## References

- [1] World Health Organization. WHO Timeline - COVID-19 [online] (Jun 2020) [cited 25 Jun 2020].
- [2] C. Sohrabi, Z. Alsafi, N. O'Neill, M. Khan, A. Kerwan, A. Al-Jabir, C. Iosifidis, R. Agha, World health organization declares global emergency: A review of the 2019 novel coronavirus (covid-19), *International Journal of Surgery* 76 (2020) 71 – 76.  
doi:<https://doi.org/10.1016/j.ijssu.2020.02.034>.  
URL <http://www.sciencedirect.com/science/article/pii/S1743919120301977>
- [3] Ministério da Saúde do Brasil. Painel coronavírus [online] (6 2020) [cited 25 Jun 2020].
- [4] World Health Organization. WHO Coronavirus Disease (Covid-19) Dashboard [online] (6 2020) [cited 25 Jun 2020].
- [5] S. Singh, K. S. Parmar, J. Kumar, S. J. S. Makkhan, Development of new hybrid model of discrete wavelet decomposition and autoregressive integrated moving average model, *Chaos, Solitons & Fractals* 135 (2020) 109866.  
doi:<https://doi.org/10.1016/j.chaos.2020.109866>.  
URL <http://www.sciencedirect.com/science/article/pii/S0960077920302666>

- [6] K. Prem, Y. Liu, T. Russell, A. Kucharski, R. Eggo, N. Davies, S. Flasche, S. Clifford, C. Pearson, J. Munday, S. Abbott, H. Gibbs, A. Rosello, B. Quilty, T. Jombart, F. Sun, C. Diamond, A. Gimma, K. Zandvoort, S. Funk, C. Jarvis, W. Edmunds, N. Bosse, J. Hellewell, M. Jit, P. Klepac, The effect of control strategies to reduce social mixing on outcomes of the covid-19 epidemic in wuhan, *The Lancet Public Health* 5 (5) (2020) e261 – e270.  
doi:[https://doi.org/10.1016/S2468-2667\(20\)30073-6](https://doi.org/10.1016/S2468-2667(20)30073-6).  
URL <http://www.sciencedirect.com/science/article/pii/S2468266720300736>
- [7] J. Hellewell, S. Abbott, A. Gimma, N. Bosse, C. Jarvis, T. Russell, J. Munday, A. Kucharski, W. Edmunds, F. Sun, S. Flasche, B. J. Quilty, N. Davies, Y. Liu, S. Clifford, P. Klepac, M. Jit, C. Diamond, H. Gibbs, K. Zandvoort, S. Funk, R. Eggo, Feasibility of controlling covid-19 outbreaks by isolation of cases and contacts, *The Lancet Global Health* 8 (4) (2020) e488–e496.  
doi:[https://doi.org/10.1016/S2214-109X\(20\)30074-7](https://doi.org/10.1016/S2214-109X(20)30074-7).  
URL <http://www.sciencedirect.com/science/article/pii/S2214109X20300747>
- [8] N. Crokidakis, Covid-19 spreading in rio de janeiro, brazil: Do the policies of social isolation really work? *Chaos, Solitons & Fractals* 136 (2020) 109930.  
doi:<https://doi.org/10.1016/j.chaos.2020.109930>.  
URL <http://www.sciencedirect.com/science/article/pii/S0960077920303295>
- [9] P. NADANOVSKY, A. P. P. d. SANTOS, Strategies to deal with the COVID-19 pandemic, *Brazilian Oral Research* 34 (00 2020).  
URL [http://www.scielo.br/scielo.php?script=sci\\_arttext&pid=S1806-83242020000100602&nrm=](http://www.scielo.br/scielo.php?script=sci_arttext&pid=S1806-83242020000100602&nrm=)
- [10] B. K. Mishra, A. K. Keshri, Y. S. Rao, B. K. Mishra, B. Mahato, S. Ayesha, B. P. Rukhaiyyar, D. K. Saini, A. K. Singh, Covid-19 created chaos across the globe: Three novel quarantine epidemic models, *Chaos, Solitons & Fractals* 138 (2020) 109928.

doi:<https://doi.org/10.1016/j.chaos.2020.109928>.

URL <http://www.sciencedirect.com/science/article/pii/S0960077920303271>

- [11] M. A. Acuña-Zegarra, M. Santana-Cibrian, J. X. Velasco-Hernandez, Modeling behavioral change and covid-19 containment in mexico: A trade-off between lockdown and com  
Mathematical Biosciences 325 (2020) 108370.  
doi:<https://doi.org/10.1016/j.mbs.2020.108370>.  
URL <http://www.sciencedirect.com/science/article/pii/S0025556420300596>
- [12] F. Wu, A. Wang, M. Liu, Q. Wang, J. Chen, S. Xia, Y. Ling, Y. Zhang, J. Xun, L. Lu, et al., Neutralizing antibody responses to sars-cov-2 in a covid-19 recovered patient cohort and their implication  
SSRN Electronic Journal (2020). doi:10.2139/ssrn.3566211.  
URL <http://dx.doi.org/10.2139/ssrn.3566211>
- [13] L. Bao, W. Deng, H. Gao, C. Xiao, J. Liu, J. Xue, Q. Lv, J. Liu, P. Yu, Y. Xu, F. Qi, Y. Qu, F. Li, Z. Xiang, H. Yu, S. Gong, M. Liu, G. Wang, S. Wang, Z. Song, Y. Liu, W. Zhao, Y. Han, L. Zhao, X. Liu, Q. Wei, C. Qin, Lack of reinfection in rhesus macaques infected with sars-cov-2, bioRxiv (2020). arXiv:<https://www.biorxiv.org/content/early/2020/05/01/2020.03.13.990226.full.pdf>.  
doi:10.1101/2020.03.13.990226.  
URL <https://www.biorxiv.org/content/early/2020/05/01/2020.03.13.990226>
- [14] D. Blanco-Melo, B. E. Nilsson-Payant, W.-C. Liu, S. Uhl, D. Hoagland, R. Møller, T. X. Jordan, K. Oishi, M. Panis, D. Sachs, T. T. Wang, R. E. Schwartz, J. K. Lim, R. A. Albrecht, B. R. tenOever, Imbalanced host response to sars-cov-2 drives development of covid-19, Cell 181 (5) (2020) 1036 – 1045.e9.  
doi:<https://doi.org/10.1016/j.cell.2020.04.026>.  
URL <http://www.sciencedirect.com/science/article/pii/S009286742030489X>
- [15] S. Pappas. After recovering from covid-19, are you immune? [online] (Jun 2020) [cited 26 Jun 2020].

- [16] N. Fernandes, Economic effects of coronavirus outbreak (covid-19) on the world economy, SSRN Electronic Journal (2020). doi:10.2139/ssrn.3557504.  
URL <http://dx.doi.org/10.2139/ssrn.3557504>
- [17] W. O. Kermack, A. G. McKendrick, G. T. Walker, A contribution to the mathematical theory of epidemics, Proceedings of the Royal Society of London. Series A, Containing Papers of a Mathematical and Physical Character 115 (772) (1927) 700–721.  
arXiv:<https://royalsocietypublishing.org/doi/pdf/10.1098/rspa.1927.0118>,  
doi:10.1098/rspa.1927.0118.  
URL <https://royalsocietypublishing.org/doi/abs/10.1098/rspa.1927.0118>
- [18] W. O. Kermack, A. G. McKendrick, G. T. Walker, Contributions to the mathematical theory of epidemics. ii. &#x2014;the problem of endemicity, Proceedings of the Royal Society of London. Series A, Containing Papers of a Mathematical and Physical Character 138 (834) (1932) 55–83.  
arXiv:<https://royalsocietypublishing.org/doi/pdf/10.1098/rspa.1932.0171>,  
doi:10.1098/rspa.1932.0171.  
URL <https://royalsocietypublishing.org/doi/abs/10.1098/rspa.1932.0171>
- [19] W. O. Kermack, A. G. McKendrick, G. T. Walker, Contributions to the mathematical theory of epidemics. iii.&#x2014;further studies of the problem of endemicity, Proceedings of the Royal Society of London. Series A, Containing Papers of a Mathematical and Physical Character 141 (843) (1933) 94–122.  
arXiv:<https://royalsocietypublishing.org/doi/pdf/10.1098/rspa.1933.0106>,  
doi:10.1098/rspa.1933.0106.  
URL <https://royalsocietypublishing.org/doi/abs/10.1098/rspa.1933.0106>
- [20] N. T. Bailey, Macro-modelling and prediction of epidemic spread at community level, Mathematical Modelling 7 (5) (1986) 689 – 717.  
doi:[https://doi.org/10.1016/0270-0255\(86\)90128-4](https://doi.org/10.1016/0270-0255(86)90128-4).  
URL <http://www.sciencedirect.com/science/article/pii/0270025586901284>
- [21] J. R. C. Piqueira, C. M. Batistela,

- Considering quarantine in the sira malware propagation model,  
 Mathematical Problems in Engineering 2019 (2019) 1–8.  
 doi:10.1155/2019/6467104.  
 URL <http://dx.doi.org/10.1155/2019/6467104>
- [22] B. Cantó, C. Coll, E. Sánchez, Estimation of parameters in a structured sir model,  
 Advances in Difference Equations 2017 (1) (2017) 33.  
 doi:10.1186/s13662-017-1078-5.  
 URL <https://doi.org/10.1186/s13662-017-1078-5>
- [23] T. W. Ng, G. Turinici, A. Danchin,  
 A double epidemic model for the sars propagation, BMC Infectious  
 Diseases 3 (1) (Sep 2003). doi:10.1186/1471-2334-3-19.  
 URL <http://dx.doi.org/10.1186/1471-2334-3-19>
- [24] A. Godio, F. Pace, A. Vergnano, Seir modeling of the italian epidemic of sars-cov-2 using computational swarm intelligence., Int. J. Environ. Res. Public Health 17 (3535) (2020).  
 doi:10.20944/preprints202004.0073.v1.
- [25] Y. Chen, J. Cheng, Y. Jiang, K. Liu,  
 A time delay dynamic system with external source for the local outbreak of 2019-ncov,  
 Applicable Analysis 0 (0) (2020) 1–12.  
 arXiv:<https://doi.org/10.1080/00036811.2020.1732357>,  
 doi:10.1080/00036811.2020.1732357.  
 URL <https://doi.org/10.1080/00036811.2020.1732357>
- [26] M. S. Abdo, K. Shah, H. A. Wahash, S. K. Panchal,  
 On a comprehensive model of the novel coronavirus (covid-19) under mittag-leffler derivative,  
 Chaos, Solitons & Fractals 135 (2020) 109867.  
 doi:<https://doi.org/10.1016/j.chaos.2020.109867>.  
 URL <http://www.sciencedirect.com/science/article/pii/S0960077920302678>
- [27] D. Fanelli, F. Piazza, Analysis and forecast of covid-19 spreading in china, italy and france,  
 Chaos, Solitons & Fractals 134 (2020) 109761.

doi:<https://doi.org/10.1016/j.chaos.2020.109761>.

URL <http://www.sciencedirect.com/science/article/pii/S0960077920301636>

- [28] R. M. Cotta, C. P. Naveira-Cotta, p. magal, Parametric identification and public health measures influence on the covid-19 epidemic evolution in bra medRxiv (2020). arXiv:<https://www.medrxiv.org/content/early/2020/05/12/2020.03.31.20049130>  
doi:10.1101/2020.03.31.20049130.  
URL <https://www.medrxiv.org/content/early/2020/05/12/2020.03.31.20049130>
- [29] C. Rothe, M. Schunk, P. Sothmann, G. Bretzel, G. Froeschl, C. Wallrauch, T. Zimmer, V. Thiel, C. Janke, W. Guggemos, M. Seilmaier, C. Drosten, P. Vollmar, K. Zwirgmaier, S. Zange, R. Wölfel, M. Hoelscher, Transmission of 2019-NCOV infection from an asymptomatic contact in Germany, *New England Journal of Medicine* 382 (10) (2020) 970–971.  
doi:10.1056/NEJMc2001468.
- [30] J. Zhang, S. Tian, J. Lou, Y. Chen, Familial cluster of COVID-19 infection from an asymptomatic, *Critical Care* 24 (1) (2020) 7–9.  
doi:10.1186/s13054-020-2817-7.
- [31] J. F. W. Chan, S. Yuan, K. H. Kok, K. K. W. To, H. Chu, J. Yang, F. Xing, J. Liu, C. C. Y. Yip, R. W. S. Poon, H. W. Tsoi, S. K. F. Lo, K. H. Chan, V. K. M. Poon, W. M. Chan, J. D. Ip, J. P. Cai, V. C. C. Cheng, H. Chen, C. K. M. Hui, K. Y. Yuen, A familial cluster of pneumonia associated with the 2019 novel coronavirus indicating person-to-person transmission, *The Lancet* 395 (10223) (2020) 514–523.  
doi:10.1016/S0140-6736(20)30154-9.  
URL [http://dx.doi.org/10.1016/S0140-6736\(20\)30154-9](http://dx.doi.org/10.1016/S0140-6736(20)30154-9)
- [32] S. Tian, N. Hu, J. Lou, K. Chen, X. Kang, Z. Xiang, H. Chen, D. Wang, N. Liu, D. Liu, G. Chen, Y. Zhang, D. Li, J. Li, H. Lian, S. Niu, L. Zhang, J. Zhang, Characteristics of COVID-19 infection in Beijing, *Journal of Infection* 80 (4) (2020) 401–406. doi:10.1016/j.jinf.2020.02.018.  
URL <https://doi.org/10.1016/j.jinf.2020.02.018>



- [33] R. Li, S. Pei, B. Chen, Y. Song, T. Zhang, W. Yang, J. Shaman, Substantial undocumented infection facilitates the rapid dissemination of novel coronavirus (sars-cov-2), *Science* 368 (6490) (2020) 489–493. arXiv:<https://science.sciencemag.org/content/368/6490/489>. doi:10.1126/science.abb3221. URL <https://science.sciencemag.org/content/368/6490/489>
- [34] K. Mizumoto, K. Kagaya, A. Zarebski, G. Chowell, Estimating the asymptomatic proportion of coronavirus disease 2019 (covid-19) cases on board the diamond princess, *Eurosurveillance* 25 (10) (Mar 2020). doi:10.2807/1560-7917.es.2020.25.10.2000180. URL <http://dx.doi.org/10.2807/1560-7917.ES.2020.25.10.2000180>
- [35] H. Nishiura, T. Kobayashi, T. Miyama, A. Suzuki, S. Jung, K. Hayashi, R. Kinoshita, Y. Yang, B. Yuan, A. R. Akhmetzhanov, N. M. Linton, Estimation of the asymptomatic ratio of novel coronavirus infections (covid-19), *medRxiv* (2020). arXiv:<https://www.medrxiv.org/content/early/2020/02/17/2020.02.03.20020248>. doi:10.1101/2020.02.03.20020248. URL <https://www.medrxiv.org/content/early/2020/02/17/2020.02.03.20020248>
- [36] L. C. Ribeiro, A. T. Bernardes, Estimate of underreporting of COVID-19 in Brazil by Acute Respiratory Syndrome, *Notas Técnicas Cedeplar-UFMG 010*, Cedeplar, Universidade Federal de Minas Gerais (Apr. 2020). URL <https://ideas.repec.org/p/cdp/tecnot/tn010.html>
- [37] N. M. Ferguson, D. Laydon, G. Nedjati-Gilani, N. Imai, K. Ainslie, M. Baguelin, S. Bhatia, A. Boonyasiri, Z. Cucunubá, G. Cuomo-Dannenburg, A. Dighe, I. Dorigatti, H. Fu, K. Gaythorpe, W. Green, A. Hamlet, W. Hinsley, L. C. Okell, S. Van Elsland, H. Thompson, R. Verity, E. Volz, H. Wang, Y. Wang, P. Gt Walker, C. Walters, P. Winskill, C. Whittaker, C. A. Donnelly, S. Riley, A. C. Ghani, Impact of non-pharmaceutical interventions (npis) to reduce covid-19 mortality and healthcare demand, *Imperial.Ac.Uk* (2020) 3–20doi:10.25561/77482.
- [38] R. Verity, L. C. Okell, I. Dorigatti, P. Winskill, C. Whittaker, N. Imai, G. Cuomo-Dannenburg, H. Thompson, P. Walker, H. Fu, A. Dighe,

- J. Griffin, A. Cori, M. Baguelin, S. Bhatia, A. Boonyasiri, Z. M. Cucunuba, R. Fitzjohn, K. A. M. Gaythorpe, W. Green, A. Hamlet, W. Hinsley, D. Laydon, G. Nedjati-Gilani, S. Riley, S. van Elsland, E. Volz, H. Wang, Y. Wang, X. Xi, C. Donnelly, A. Ghani, N. Ferguson, Estimates of the severity of covid-19 disease, medRxiv (2020).  
 arXiv:<https://www.medrxiv.org/content/early/2020/03/13/2020.03.09.20033357.full.pdf>,  
 doi:10.1101/2020.03.09.20033357.  
 URL <https://www.medrxiv.org/content/early/2020/03/13/2020.03.09.20033357>
- [39] J. Guckenheimer, P. Holmes, Nonlinear Oscillations, Dynamical Systems, and Bifurcations of Vector Fields, 2nd Edition, Vol. 42 of Applied Mathematical Sciences, Springer, 1983.
- [40] M. W. Hirsch, S. Smale, Differential Equations, Dynamical Systems, and Linear Algebra, Vol. 1, Academic Press, New York, 1974.
- [41] SEADE. SP contra o novo coronavírus boletim completo [online] (6 2020) [cited 19 Jun 2020].
- [42] P. Kellam, W. Barclay, The dynamics of humoral immune responses following SARS-CoV-2 infection and Journal of General Virology (2020) jgv001439doi:10.1099/jgv.0.001439.  
 URL <https://www.microbiologyresearch.org/content/journal/jgv/10.1099/jgv.0.001439>
- [43] K. A. Callow, H. F. Parry, M. Sergeant, D. A. Tyrrell, The time course of the immune response to experimental coronavirus infection of man, Epidemiology and Infection 105 (2) (1990) 435–446.  
 doi:10.1017/S0950268800048019.  
 URL </core/journals/epidemiology-and-infection/article/time-course-of-the-immune-respon>
- [44] H. Mo, G. Zeng, X. Ren, H. Li, C. Ke, Y. Tan, C. Cai, K. Lai, R. Chen, M. Chan-Yeung, N. Zhong, Longitudinal profile of antibodies against SARS-coronavirus in SARS patients and their clinical significance Respiriology 11 (1) (2006) 49–53. doi:10.1111/j.1440-1843.2006.00783.x.  
 URL </pmc/articles/PMC7192223/?report=abstracthttps://www.ncbi.nlm.nih.gov/pmc/articles/>

- [45] J. P. Moore, P. J. Klasse, SARS-CoV-2 vaccines: 'Warp Speed' needs mind melds not warped minds., *Journal of virology* (June) (2020). doi:10.1128/JVI.01083-20.  
URL <http://www.ncbi.nlm.nih.gov/pubmed/32591466>
- [46] J. Seow, C. Graham, B. Merrick, S. Acors, K. J. A. Steel, O. Hemmings, A. O'Byrne, N. Kouphou, S. Pickering, R. Galao, G. Betancor, H. D. Wilson, A. W. Signell, H. Winstone, C. Kerridge, N. Temperton, L. Snell, K. Bisnauthsing, A. Moore, A. Green, L. Martinez, B. Stokes, J. Honey, A. Izquierdo-Barras, G. Arbane, A. Patel, L. OConnell, G. O Hara, E. MacMahon, S. Douthwaite, G. Nebbia, R. Batra, R. Martinez-Nunez, J. D. Edgeworth, S. J. D. Neil, M. H. Malim, K. Doores, Longitudinal evaluation and decline of antibody responses in SARS-CoV-2 infection, *medRxiv* (2020) 2020.07.09.20148429doi:10.1101/2020.07.09.20148429.  
URL <http://medrxiv.org/content/early/2020/07/11/2020.07.09.20148429.abstract>
- [47] A. W. Edridge, J. M. Kaczorowska, A. C. Hoste, M. Bakker, M. Klein, M. F. Jebbink, A. Matser, C. Kinsella, P. Rueda, M. Prins, P. Sastre, M. Deijs, L. van der Hoek, Coronavirus protective immunity is short-lasting, *medRxiv* (2020) 2020.05.11.20086439doi:10.1101/2020.05.11.20086439.  
URL <https://www.medrxiv.org/content/10.1101/2020.05.11.20086439v2>
- [48] R. Li, S. Pei, B. Chen, Y. Song, T. Zhang, W. Yang, J. Shaman, Substantial undocumented infection facilitates the rapid dissemination of novel coronavirus (SARS-CoV2), *Science* (New York, N.Y.) 493 (May) (2020) 489–493. doi:10.1126/science.abb3221.
- [49] W. Wang, J. Tang, F. Wei, Updated understanding of the outbreak of 2019 novel coronavirus (2019-nCoV) in Wuhan, China, *Journal of Medical Virology* 92 (4) (2020) 441–447. doi:10.1002/jmv.25689.
- [50] S. Mehrotra, On the implementation of a primal-dual interior point method, *SIAM Journal on Optimization* 2 (4) (1992) 575–601.

arXiv:<https://doi.org/10.1137/0802028>, doi:10.1137/0802028.

URL <https://doi.org/10.1137/0802028>

- [51] M. C. Bartholomew-Biggs, Recursive quadratic programming methods based on the augmented lagrangian, *Computation Mathematical Programming* (1987) 21–41 doi:10.1007/bfb0121177.  
URL <http://dx.doi.org/10.1007/BFb0121177>
- [52] A. R. Conn, N. I. M. Gould, P. L. Toint, Trust Region Methods, Society for Industrial and Applied Mathematics, 2000.  
arXiv:<https://epubs.siam.org/doi/pdf/10.1137/1.9780898719857>,  
doi:10.1137/1.9780898719857.  
URL <https://epubs.siam.org/doi/abs/10.1137/1.9780898719857>
- [53] C. Moler, Numerical Computing with MATLAB, Other titles in applied mathematics, Society for Industrial and Applied Mathematics, 2004.
- [54] SEADE. Portal estatísticas do Estado de São Paulo [online] (6 2020) [cited 19 Jun 2020].

This figure "BirthDeathRate.png" is available in "png" format from:

<http://arxiv.org/ps/2007.01295v3>

This figure "SocialDistMeasure.png" is available in "png" format from:

<http://arxiv.org/ps/2007.01295v3>